

An All-Silicon Single-Wafer Fabrication Technology for Precision Microaccelerometers

Navid Yazdi and Khalil Najafi
Center for Integrated Sensors and Circuits
University of Michigan, Ann Arbor, MI 48019, USA

SUMMARY

This paper reports a novel all-silicon single-wafer fabrication technology for high precision capacitive accelerometers. This technology combines both surface and bulk micromachining to attain a large proofmass, controllable/small damping, and a small airgap for large capacitance variation. The microfabrication process provides large proofmass by using the whole wafer thickness, and a large sense capacitance by utilizing a thin sacrificial layer. The sense/feedback electrodes are formed by a deposited $2\mu\text{m}$ polysilicon film with embedded $20\text{-}30\mu\text{m}$ thick vertical stiffeners. These electrodes, while thin, are made very stiff by the thick embedded stiffeners so that force rebalancing of the proofmass becomes possible. The polysilicon electrodes are patterned to create damping holes. Several prototype microaccelerometers are fabricated successfully. Sensitivity of the devices with $2\text{mm} \times 1\text{mm}$ proofmass and full-bridge support are measured to be 2pF/g .

Keywords: Inertial sensors, μg accelerometer, Fabrication technology.

INTRODUCTION

High precision accelerometers are widely used in applications such as inertial navigation, microgravity measurements and seismology. Recent advances in fabrication technologies for microaccelerometers have made mass production of these devices with low/medium sensitivities possible [1]. However, to date only a few precision μg silicon accelerometers are reported; they all use multiple wafer bonding as part of their fabrication process [2-4]. These devices achieve high resolution by using a thick and large proofmass. However, their damping is not easily controlled due to difficulties in forming damping holes in thick proofmass and electrodes. Furthermore, multiple wafer bonding is not desirable due to process difficulties or thermal expansion mismatches. Surface micromachined accelerometers [5] have the main advantages of being monolithically fabricated with the interface circuit and achieving high Q-factor by forming damping holes in the proofmass. However, the proofmass in these devices is small which results in higher mechanical noise floor and reduced signal pick up.

This paper presents a novel single-wafer all-silicon microfabrication technology for high precision microaccelerometers which is based on combined surface and bulk micromachining. This technology overcomes all the shortcomings of bulk and surface micromachining- it facilitates fabrication of devices with large proofmass, controllable/small damping, and large capacitance variation which are the key

factors for attaining μg and sub- μg resolution in capacitive accelerometers.

μg ACCELEROMETER ISSUES

A precision microaccelerometer is typically operated closed-loop to obtain higher bandwidth, full-scale range, and linearity. Therefore the main design consideration for these devices is meeting the resolution specification. Resolution of a microaccelerometer is determined by its mechanical and readout electronics noise. Mechanical noise can be reduced by increasing the size of the proofmass and increasing its Q-factor. Electrical signal-noise ratio can be improved by reducing electronic noise, and increasing proofmass and device capacitance variation. The latter two provide a larger signal pick-up and result in less stringent readout circuit requirements.

Mechanical noise is mainly due to Brownian motion and can be expressed in terms of mass size and total damping [6]. The key element in obtaining low mechanical noise floor without any need for vacuum packaging is increasing mass size and reducing the damping coefficient simultaneously. Figure 1 shows the Total Noise Equivalent Acceleration (TNEA) versus the proofmass thickness at atmospheric pressure for three different cases: (a) $4\mu\text{m}$ damping holes with $9\mu\text{m}$ pitch, (b) $5\mu\text{m}$ damping holes with $15\mu\text{m}$ pitch, (c) without any damping holes. The device has a mass/electrode area of $2\text{mm} \times 1\text{mm}$ and $1.5\mu\text{m}$ gap. The squeeze film damping is assumed to be dominant and relations presented in [6-7] are used for the noise and damping coefficient calculations. As can be observed μg noise floor is only achievable by using both thick proofmass

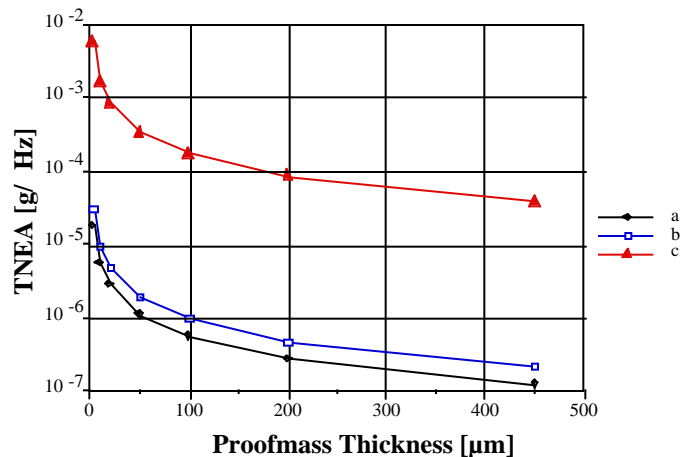


Figure 1: Total Noise Equivalent Acceleration (TNEA) due to Brownian motion at atmospheric pressure for an accelerometer with $1\text{mm} \times 2\text{mm}$ mass/electrode area and $1.5\mu\text{m}$ air gap with (a) $4\mu\text{m}$ damping holes with $9\mu\text{m}$ pitch, (b) $5\mu\text{m}$ damping holes with $15\mu\text{m}$ pitch, (c) no damping holes.

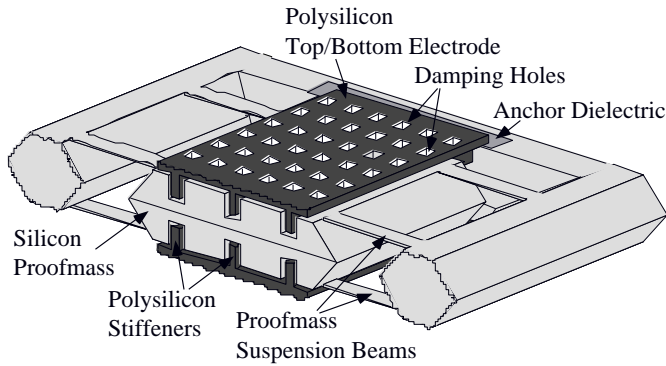


Figure 2: Microaccelerometer structure.

and damping holes. Note that using small damping holes results in almost no loss of capacitance since the fringing capacitance becomes comparable with the lost capacitance due to reduction in surface area.

The open loop sensitivity of the accelerometer increases linearly with increasing proofmass thickness and electrode area. It is also inversely proportional to the air gap squared. Therefore, the electrical signal-noise ratio can be improved by forming a thick large mass and small air gap. For instance, for the aforementioned device with $450\mu\text{m}$ thick proofmass and four $700\mu\text{m} \times 40\mu\text{m} \times 3\mu\text{m}$ cantilever supports, a rest capacitance of 10pF and capacitance variation of over 100pF/g can be obtained, which with a readout circuit resolution of 0.1fF results in μg performance.

MICROACCELEROMETER STRUCTURE

Our approach to addressing all the μg accelerometer design issues is to combine both surface and bulk micromachining in order to achieve high device sensitivity, low noise floor, and controllable damping - all by using a single silicon wafer. The central idea behind the process is to use the whole wafer thickness to attain a large proofmass, to utilize a sacrificial thin film to form a uniform and conformal gap over a large area, and to create electrodes by depositing polysilicon on the wafer. These electrodes, while thin, are made very stiff by embedding thick vertical stiffeners in them so that force rebalancing of the proofmass becomes possible. The technology utilizes a trench refill technique to form thick stiffeners by depositing thin polysilicon films. Any damping hole configuration and geometry can be easily formed on the poly electrodes to optimize damping coefficient and capacitance, while there is no concern with large hole density and its effect on the electrode softening as the plate stiffness is mainly provided by the embedded stiffeners.

Figure 2 shows the device structure obtained by this technology. The proofmass and its supporting rim are formed by bulk micromachining and have the whole wafer thickness. There are eight boron doped suspension beams which are symmetric with respect to the proofmass centerline and result in low cross-axis sensitivity. The electrodes are polysilicon plates created on both sides of the proofmass and anchored on an isolation dielectric at the frame. Furthermore, the device has low temperature sensitivity as the poly electrodes and silicon frame expansion coefficients match each other closely.

After completion of fabrication the microaccelerometer is mounted on one edge of its frame on a recessed substrate and is suspended over the recessed area. In this manner the package and mounting induced stresses will be reduced and not affect the device performance. The device has bonding pads on both sides. Each pad at the bottom has a metal overhang over the frame which is directly bonded to the pads on the mounting substrate using ultrasonic wirebonder and provide beam-lead transfer. Access to the top pads is provided by direct wire-bonding to them.

STRUCTURE AND SYSTEM SIMULATION

The feasibility of realizing high precision accelerometers fabricated by the presented technology has been investigated and verified thoroughly by combined FEM analysis using ABAQUS and electromechanical system simulation using SIMULINK and MATLAB. The microaccelerometer is assumed to be operated in a sigma-delta modulation loop which provides a wide dynamic-range direct digital output. The actual mechanical parameters of the structure including electrode stiffness were obtained by FEM analysis and fed into the SIMULINK model. The SIMULINK model is based on a second order mass-damping-spring system for all mechanical structures, and continuous/discrete time transfer functions for the readout electronics and closed-loop sigma-delta modulation blocks. All the required digital signal processing operations for the sigma-delta output bit-stream are implemented with MATLAB functions.

Simulations have revealed that as long as the electrode stiffness is above a certain threshold, which is a function of proofmass size and suspension spring constant, the accelerometer servo system is stable. This threshold is easily achievable in the proposed technology by using $20\mu\text{m}$ deep trenches. Furthermore, high resolution and precision from the overall system, including low harmonic-distortion, is attainable without any need for very deep trenches. For instance Figure 3 shows the simulated response of a closed loop accelerometer to $10\mu\text{g}$ input acceleration on top of a 1g bias. The microaccelerometer has a plate area of $2000\mu\text{m} \times 2000\mu\text{m}$, $1.5\mu\text{m}$ gap, 10 stiffeners each $3\mu\text{m}$ wide and $25\mu\text{m}$ deep. As can be observed the signal is recovered using digital filtering

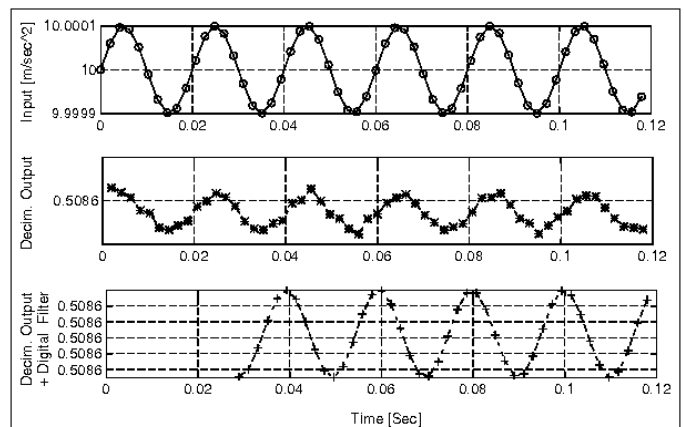


Figure 3: Simulated response of the microaccelerometer to $10\mu\text{g}$ input acceleration on top of 1g DC bias.

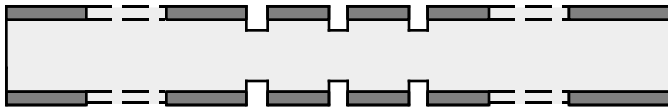
which is implemented as part of the signal processing needed for the sigma-delta modulation control loop. The large signal response of the system to a 1g input sinusoidal acceleration shows less than 1% total harmonic distortion.

FABRICATION PROCESS

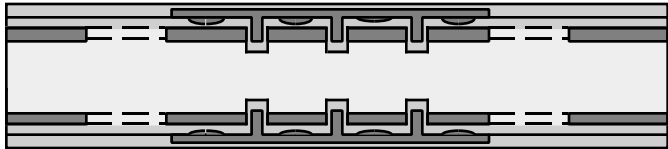
The fabrication process requires eight masks, and is performed symmetrically on both sides of the wafer, as shown in Figure 4. The process starts with a shallow ($3\mu\text{m}$) p++ boron diffusion on $\langle 100 \rangle$ double-polished p-type Si wafer, using thermal oxide as a mask. Both sides of the wafer are patterned and the patterns are aligned to each other. The shallow boron diffusion is performed at 1150°C for 30min and defines the beams, the proofmass and the supporting rim. Then, 900\AA of LPCVD nitride is deposited and patterned to form the poly electrode anchors and isolation dielectric under the electrode dimples. The next masking step is etching $20\text{-}30\mu\text{m}$ deep, $6\mu\text{m}$ wide trenches to define the vertical electrode stiffeners. The deep trench etch is performed by



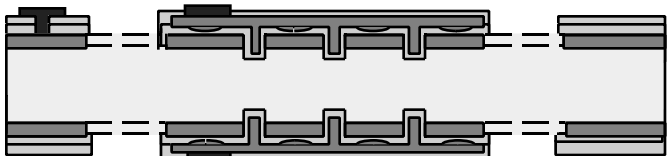
(a) Shallow boron diffusion to define beams, proofmass, and supporting rim. Nitride deposition and definition for electrode anchors and isolation dielectric underneath electrode dimples.



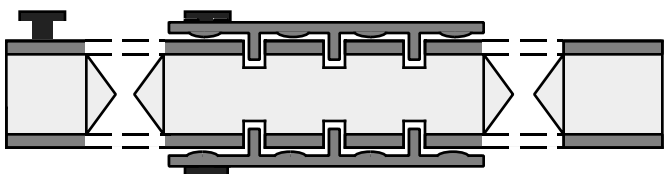
(b) Trench etch for vertical electrode stiffener definition.



(c) Trench refill using LPCVD sacrificial oxide and poly. Poly patterning to form electrodes and damping holes. Poly is sealed by a top LPCVD oxide layer. Dimples inside poly electrode are created by partial etching of the sacrificial oxide before poly deposition.



(d) Contact opening, metal deposition and patterning



(e) Proofmass and rim formation by etching in EDP. Final proofmass release by etching the sacrificial oxide.

Figure 4: Fabrication process sequence of a μg accelerometer.

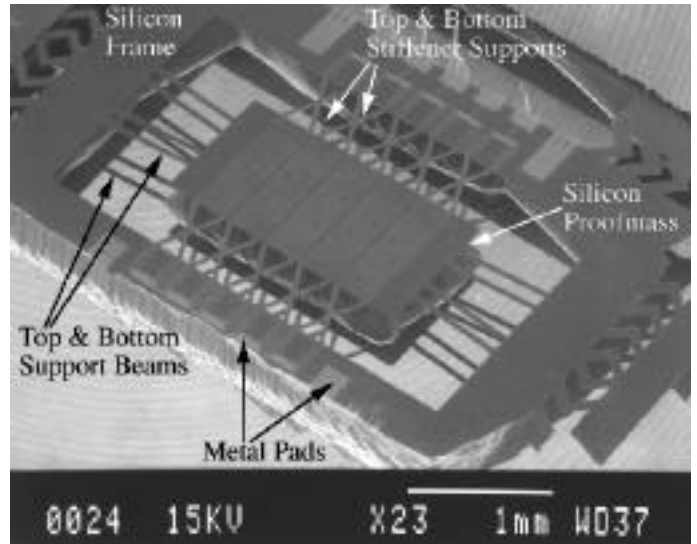


Figure 5: SEM view of a high-precision μg accelerometer with $2\text{mm} \times 1\text{mm}$ proofmass.

Electron Cyclotron Resonance (ECR) dry etch using Chlorine as the reacting gas and $1.8\text{-}2\mu\text{m}$ electroplated nickel as a mask.

The trenches are then refilled completely using $1.4\mu\text{m}$ sacrificial LPCVD oxide and $1.8\mu\text{m}$ LPCVD polysilicon. The polysilicon is etched back using a blanket RIE etch, exposing the sacrificial oxide and leaving poly plugs in the trenches. In this manner the step heights due to the trench etch is reduced and sacrificial oxide at the bottom of the trenches is protected. Next two patterning steps are performed on the sacrificial oxide. First, it is patterned and partially wet-etched to form dimples inside the poly electrodes. These dimples reduce the contact area and help reduce stiction. Second, narrow strips of sacrificial oxide are patterned and etched away at the anchors. Sacrificial oxide is left in most areas of the anchors to reduce the parasitics and is sealed between underneath nitride and top poly. A $2\mu\text{m}$ LPCVD polysilicon is then deposited to connect to the plugs in the trenches and form the electrodes. The poly electrode is doped with phosphorus half way through deposition. The electrodes are sealed with a 4000\AA LPCVD oxide in the next step. This oxide is patterned to form metal contacts and openings to bulk Si for the subsequent proofmass release. The wafer is then patterned for Cr/Au ($400\text{\AA}/5000\text{\AA}$) sputtering and lift-off. The proofmass is released by an EDP etch at 110°C and subsequent sacrificial oxide etch in 1:1 HF:DI-water. Then the released structures are coated with Self-Assembled Monolayer (SAM) and dried in oven. SAM coating makes the poly and silicon surfaces hydrophobic and helps substantially with avoiding stiction.

FABRICATION RESULTS

A number of prototype microaccelerometers have been successfully fabricated using the presented technology. Figure 5 shows a SEM view of the device with $2\text{mm} \times 1\text{mm}$ proofmass. A rectangular proofmass has been utilized for this device to achieve a large mass without making the electrodes too long. The device has 5 electrically isolated electrodes on each side which are anchored at the rim using stiffened poly supports. An enlarged view of a single electrode stiffener

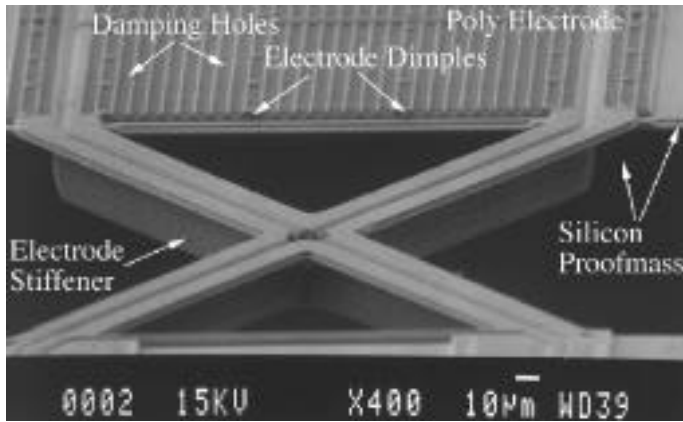


Figure 6: An enlarged view of single electrode stiffener support. The electrode damping holes and electrode dimples can be seen.

support is shown in Figure 6. The electrode damping holes and electrode dimples can also be seen in this figure. These dimples reduce the effective contact area of electrode and proofmass, and hence help with reducing stiction. A close-up view of the cross-section of proofmass and stiffened poly electrode is shown in Figure 7. As can be seen the air gap separates the electrode stiffener from the proofmass.

Figure 8 shows the measured open-loop response of a microaccelerometer with 2mm x 1mm proofmass and 16 suspension beams in a full-bridge configuration. The device shows a sensitivity of 2pF/g which is much less than the sensitivity of a device with cantilever support since the intrinsic stress of p++ beams increases the proofmass suspension spring constant significantly in a bridge configuration. Electrostatic force is used to generate input acceleration in this measurement. Small displacement of the electrodes is taken into account in these tests by measuring spring constant of the electrode independently using the included test structures.

CONCLUSION

A novel all silicon microfabrication process for high

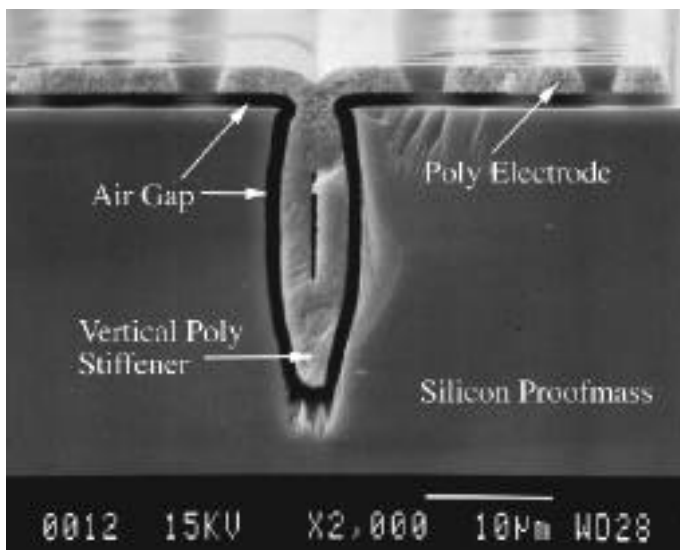


Figure 7: A cross-sectional close-up of the proofmass and stiffened poly electrode.

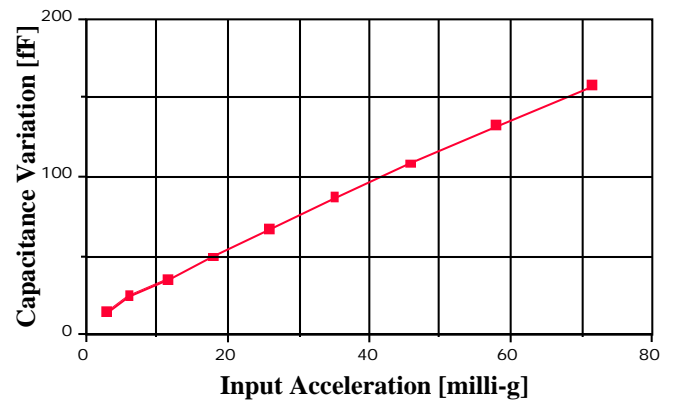


Figure 8: Open-loop response of microaccelerometer with 2mm x 1mm proofmass and full-bridge support.

precision accelerometer is presented in this paper. This technology overcomes all the μg accelerometer design challenges by combining both surface and bulk micromachining in order to achieve high device sensitivity, low noise floor, and controllable damping - all by using a single wafer process. Feasibility of achieving μg performance is verified through extensive simulations and prototype devices are fabricated successfully. Sensitivity of the devices with 2mm x 1mm proofmass and full-bridge support are measured to be 2pF/g, and is expected to be much higher for the devices with cantilever support.

ACKNOWLEDGMENTS

The authors would like to thank W.H. Juan for deep ECR trench etches and K. Handique for SAM coating. This work was supported by the Defense Advanced Research Projects Agency under contract JFBI 92-149, and in part by NSF-NYI grant #ECS-925 7400.

REFERENCES

- [1] Analog Devices, "ADXL05-Monolithic Accelerometer with Signal Conditioning," Datasheet, 1995.
- [2] W. Henrion, et. al., "Wide Dynamic Range Direct Digital Output Accelerometer," *Digest, Solid-State Sensor and Actuator Workshop*, pp. 153-157, Hilton-Head Island, SC, June 1990.
- [3] Y. de Coulon, et. al., "Design and Test of a Precision Servoaccelerometer with Digital Output," *Proc. Transducers 93*, pp. 832-835, Yokohama, Japan, June 1993.
- [4] K. Warren, "Navigation Grade Silicon Accelerometer with Sacrificially Etched SIMOX and BESOI Structure," *Digest, Solid-State Sensor and Actuator Workshop*, pp. 69-72, Hilton-Head Island, SC, June 1994.
- [5] B.E. Boser and R. T. Howe, "Surface Micromachined Accelerometers," *IEEE Journal of Solid-State Circuits*, vol. 31, pp. 366-375, March 1996.
- [6] T. Gabrielson, "Mechanical-Thermal Noise in Micro-Mechanical Acoustic and Vibration Sensors," *IEEE Trans. on Electron Devices*, vol. 40, pp. 903-909, May 1993.
- [7] V.M. McNeil, M. Novack, M.A. Schmidt "Design and Fabrication of Thin-Film Microaccelerometer using Wafer Bonding," *Proc. Transducers 93*, pp. 822-825, Yokohama, Japan, June 1993.